Article:

True bridging liquid-solid ratio (TBSR): Redefining a critical process parameter in spherical agglomeration

Jonathan D. Tew, Kate Pitt, Rachel Smith, James D. Litster [*]

Department of Chemical and Biological Engineering, The University of Sheffield, Mappin Street, Sheffield S1 3JD, UK

HIGHLIGHTS

- Bridging liquid-solid ratio (BSR) is a crucial parameter in spherical agglomeration.
- BSR does not account for bridging liquid-solvent miscibility.
- A new term, True BSR, is introduced to account for miscibility.
- Experimental validation supports the rationale of the definition.
- TBSR provides a quick, accurate comparison tool for different solvent systems.

GRAPHICAL ABSTRACT

ARTICLE INFO

ABSTRACT

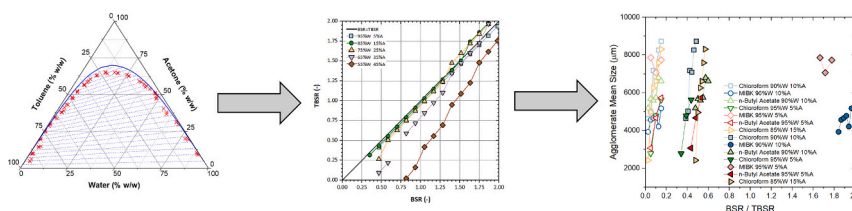Spherical agglomeration of crystals via addition of an immiscible bridging liquid can improve active pharmaceutical ingredient handling and tabletability. Bridging liquid amount is quantified by the bridging liquid-solid ratio (BSR). However, the optimal range of the BSR for agglomerates to form is highly dependent on the bridging liquid/solvent/antisolvent system. Here, a new definition is introduced to account for bridging liquid-solvent miscibility; true bridging liquid-solid ratio (TBSR). A method for calculating TBSR from the system ternary phase diagram is demonstrated for five different common binder liquids with acetone/water as the solvent/antisolvent system. Results show the value of BSR varies dramatically for a given TBSR as a function of both the system and the solids loading. Experimental salicylic acid agglomeration studies confirm optimal BSR varied widely with binder liquid and solids loading between 0.2 and 2, but the optimum TBSR for all experiments was in a narrow range between 0.05 and 0.15. Thus, TBSR is a robust dimensionless parameter for design and scale up of spherical agglomeration processes.

1. Introduction

Spherical agglomeration is a technique which allows the crystallisation and agglomeration of high value products, either simultaneously or in sequence, yielding improvements in micromeritic and functional properties required for subsequent downstream processing [1]. In the case of the active pharmaceutical ingredients (APIs), it is necessary for agglomerates to have the required properties to ensure tabletting is successful. This includes, but is not limited to, a pre-determined mean size with a narrow size distribution, good compressibility, and the ability to be combined with excipients [2–4]. Spherical agglomeration of crystals with difficult morphologies may allow direct compression to be used for solid dosage form manufacture, avoiding more costly routes including wet or dry granulation.

Spherical agglomeration applied to anti-solvent crystallisation processes requires three key liquids; a solvent in which the API is dissolved; an anti-solvent to precipitate the crystals; an immiscible bridging liquid to agglomerate the crystals [1]. The bridging liquid must preferentially wet the crystals of interest. To maximise the degree of agglomeration of the particle of interest, it is preferable to work in the immiscible region of the ternary phase diagram for the solvent system. This provides a much greater degree of control of the process.

The size of initial crystals and the bridging liquid droplets determines the three key rate processes in spherical agglomeration; wetting and nucleation; growth and consolidation; breakage and attrition. These same mechanisms are also recognised in wet granulation [5]. If the bridging liquid droplets are larger than the initial crystals of interest, an immersion mechanism occurs during wetting [6]. Here, crystals penetrate the droplets and agglomerate within the droplets themselves. The distribution mechanism occurs when the crystals of interest are larger than the bridging liquid droplets. The crystals are coated by the droplets which allows them to agglomerate over time [6]. Agglomerates formed by the immersion mechanism have been found to be much more spherical, denser, and larger compared to their counterparts formed by the distribution mechanism [7,8].

A full review of the mechanisms and parameters involved in spherical agglomeration is available in the literature [9]. The majority of research in spherical agglomeration has been experimentally focused, evaluating the influence of process and formulation parameters in particular, on subsequent agglomerate characteristics [10–14]. An overview of these studies is given in Table 1.

Table 1
A summary of the influence of process and formulation parameters on spherical agglomerates.

Parameter	Influence	Reference
Bridging Liquid-Solid Ratio (BSR)	Increase in critical range, increase in mean size	[15,16]
	Above the critical range, poor mechanical robustness	[17,18]
	Below the critical range, decrease in mean size, fines in solution	[17,18]
Temperature	Influences crystal growth during crystallisation	[19]
	Increase leads to larger agglomerates	[19]
	Increases may improve bulk density	[4]
Agitation Speed	Moderate increases promote agglomeration and mean size	[20]
	Further increases promote breakage, decreasing mean size	[4,16,21]
	Can be used to tailor mechanical properties	[16,21]
Residence Time	Increases lead to larger agglomerates	[22]
	Sphericity and strength improved with longer times	[15,16]
	Increases in time; higher density; reduced porosity	[14,16]
Solvent Addition Method	Addition of solvent with crystals; increased sphericity	[19]
	Rate of bridging liquid infusion produces unclear effects	[7,10]
	Can lead to the formation of different polymorphs	[23]
	Simultaneous procedure improves mechanical properties	[23,24]
Bridging Liquid Properties	Higher wetting of solids produces larger agglomerates	[17]
	Increased feed rate leads to a smaller agglomerate mean size	[15]
	Slower feed rates preserve bridging liquid droplet size	[7]
Primary Crystals	Smaller mean size produces mechanically robust agglomerates	[7,8]
	Low solubility in anti-solvent increases mean agglomerate size	[15]

Of these parameters, the bridging liquid-solid ratio (BSR) is considered to be the most important. Within the literature, the bridging liquid is currently quantified by a volume ratio, the bridging liquid-solid ratio:

$$BSR = \frac{V_z}{V_s} \tag{1}$$

where V_z volume of liquid binder added and V_s is the volume of the solid (crystalline) phase in the system. Previous studies have found a 'critical' range for the BSR [16,17]. Operating below this critical range usually produces agglomerates which are friable and small in size, as many crystals remain un-agglomerated as fines within the bulk solution. Above the critical range, agglomerates tend to form a paste. Within the critical range, agglomerates are well-formed, with a high density and low porosity, as most fines are incorporated. All three of these conditions are shown in Fig. 1 for the immersion nucleation mechanism. Increases in the BSR within the critical range are often shown to produce improvements in key properties of agglomerates, including size, size distribution and mechanical strength [15,16]. Generally, it is preferential for a specific size to be reached, usually in the region of 200–500 μm, which is comparable with the excipients used in formulation [25,26]. A narrow size distribution ensures the dissolution profile of the API remains predictable, whilst mechanical strength is important to guarantee tablet structure and formation.

In this respect, there are clear parallels between spherical agglomeration and wet granulation; a lack of granulation in low binder environments; a slurry or paste formation with high binder additions; a critical range of binder-solid ratio, within which an increase results in larger granules being formed. In spherical agglomeration, the critical BSR range has previously been documented for several solvent systems, but there is no clear method for calculating this other than through time-consuming experimental observation [15–18]. The range is often found by trial and error, with no clear starting point for preliminary investigations. Furthermore, it is unclear whether the critical range holds if a different solid of interest is used within the same liquid system, as most studies observe only one solid of interest. If one of the three liquids is changed, the critical range has been shown not to hold [18,28].

Granulation studies have previously highlighted pore saturation as a critical parameter in granule growth and consolidation [29,30]. The pore saturation here is defined as the volume fraction of voids within the granule which are filled with binder. A relationship between the degree of pore saturation and the mean size of calcium hydrogen phosphate granules has previously been observed, where all systems collapsed onto one curve, regardless of the type of binder that was used (Fig. 2a) [5]. Fig. 2b demonstrates that similar trends were found in spherical agglomeration, with an increase in the agglomerate size with BSR within the critical BSR range [5,9,15–18]. However, not all these systems lie along a single curve, as in wet granulation. As a result, prediction of the agglomerate size from a given BSR value is currently not possible.

The current BSR definition only accounts for the initial volume of both the bridging liquid and solid added. The BSR definition assumes that there is, in fact, complete immiscibility between the bridging liquid and the other solvents utilised. Consequently, the full bridging liquid volume added to the process is assumed to be available to agglomerate the crystals of interest. In typical pharmaceutical systems, however, this is not true. Analysis of the ternary phase diagram of the system is necessary to allow the degree of solvent miscibility to be evaluated. Whilst some studies have used the ternary phase diagram to identify a suitable operating region for agglomeration, no studies have exclusively looked at the influence of solvent system miscibility [18,32–35].

Evaluation of system miscibility can be achieved through identification of the boundary between the miscible and immiscible regions, i.e. a homogenous solution or two distinct phases, respectively. An example of a ternary phase diagram is shown in Fig. 3. Water is most commonly employed as the anti-solvent and always has a degree of miscibility with the solvent, which is often ethanol or acetone [1,15,18,35,36]. Both
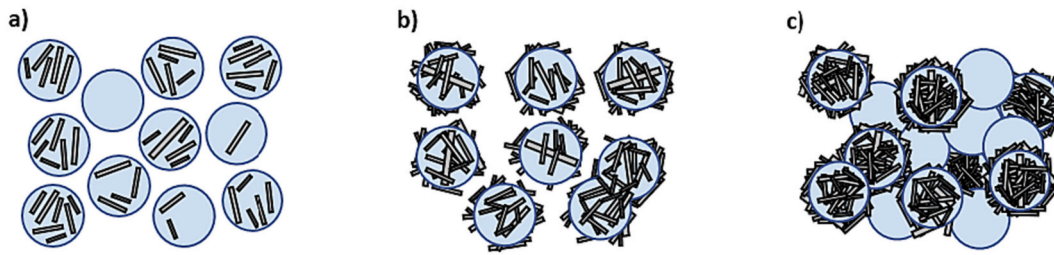
Fig. 1. The influence of a BSR value **(a)** below, **(b)** within and **(c)** above the critical range on agglomerates produced by the immersion mechanism. Adapted from Petela (1991) and Peña & Nagy (2015) [6,27].
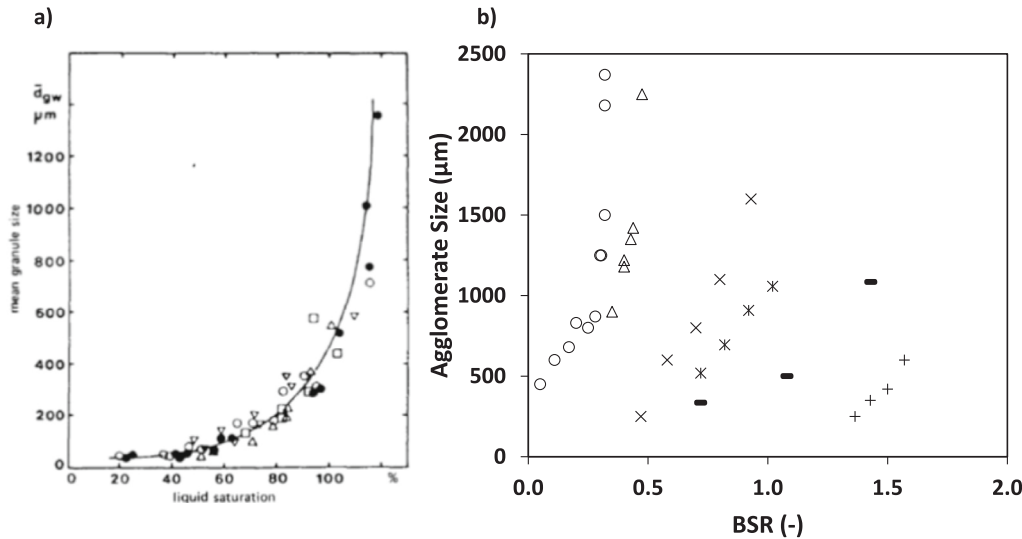

Fig. 2. (a) Granule size as a function of pore saturation for calcium hydrogen phosphate using different binders. Source: Iveson et al. [5]. **(b)** Agglomerate size as a function of bridging liquid-solid ratio for different spherical agglomeration systems: o kerosene/CaCO$_3$ [31]; Δ chloroform/salicylic acid [16]; × toluene/benzoic acid [18]; − hexane/lobenzarit disodium [17]; + dichloromethane/atorvastatin calcium [23]. Source: Pitt et al. [9].

ethanol and acetone, and most other organic solvents utilised as the solvent, have limited miscibility with the bridging liquid. Thus, when operating in the immiscible region, some bridging liquid is transferred to the first of the immiscible phases. This can be referred to as the bridging liquid poor phase, as only very small quantities of bridging liquid are present. The composition of this phase can easily be identified using Point A (x) in Fig. 3.

Additionally, both anti-solvent and solvent are transferred from the bridging liquid poor phase into the second immiscible phase, which we refer to as the bridging liquid rich phase. This phase has an entirely different composition; high quantities of the bridging liquid and small quantities of the solvent and anti-solvent. The phase composition here can be identified from Point B (☆) in Fig. 3. As the crystals are preferentially wet by the bridging liquid, we assume that agglomeration can only occur via the bridging liquid-rich phase. Critically, only the volume of this bridging liquid rich phase may agglomerate the solid of interest.

Generally, the BSR is cited as one of, if not, the most critical process controlling parameters [6,9,15–18]. The BSR is often regarded as dictating whether dense, spherical agglomerates with robust mechanical properties can be yielded from the process. However, this definition is inherently flawed, as it fails to account for the influence of liquid miscibility. It is also not standardised across current research.

In this paper, a new definition, the True BSR (TBSR), is introduced to account for miscibility, with the aim of standardising bridging liquid-solid ratio reporting. A combined approach of experimental and computational work is used to determine the ternary phase diagram of water-acetone-bridging liquid systems. This approach is used to reduce the required experimental work in determining ternary phase diagrams,

whilst partially validating existing thermodynamic models. The relationship between BSR and TBSR is explored for several systems, and validated through experimental agglomeration studies.

2. Theory – True BSR definition

As shown in Fig. 3, the anti-solvent is denoted X, solvent Y and bridging liquid Z. X and Y are fully miscible, whilst Z is selected for its immiscibility with the X-Y mixture. If we plot the X-Y-Z ternary phase diagram, a significant two-phase region exists. Here, a solvent rich continuous phase forms, and a bridging liquid rich discrete phase. The definition of the bridging liquid-solid ratio is given as:

$$BSR = \frac{V_Z}{V_S} = \frac{\frac{M_Z}{\rho_Z}}{\frac{M_S}{\rho_S}} \qquad (2)$$

where the mass of solid within the system is M_S, and the mass of three liquid components in the system, on a solids free basis, is M_X, M_Y and M_Z respectively. The true density of the bridging liquid and solid is represented as ρ_Z and ρ_S respectively. Provided that the masses of each liquid component is given, the ternary phase diagram can be used to identify the system conditions. If the system lies within the immiscible two-phase region, the tie-lines can be interpolated to give the composition of the discrete phase and the continuous phase. These can be given as x_X, x_Y, x_Z and y_X, y_Y, y_Z respectively. A mass balance on any of the three liquid components allows the mass fraction of the bridging liquid-rich phase to be calculated:
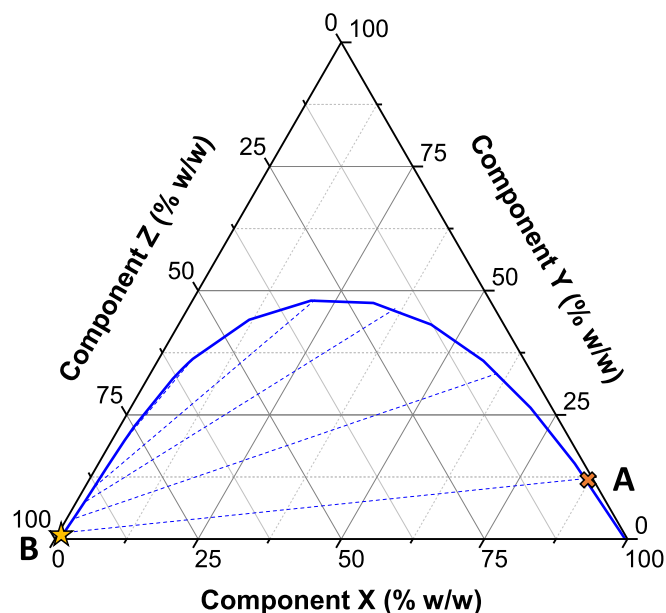
Fig. 3. An example Aspen ternary phase diagram plotted in Origin Pro. The blue line indicates the boundary between miscible (above) and immiscible (below) regions. Dashed lines show the tie-lines of the system. Point A (x) represents the composition of the bridging liquid poor phase. Point B (☆) provides the composition of the bridging liquid rich phase.

(For interpretation of the references to colour in this figure legend, the reader is referred to the web version of this article.)

$$M_Z = x_Z M_D + y_Z(M_T - M_D) \qquad (3)$$

where M_D represents the mass fraction of the bridging liquid-rich phase. M_T represents the total system mass:

$$M_T = M_X + M_Y + M_Z \qquad (4)$$

The well-known Inverse Lever Rule can be obtained if we rearrange eq. 3:

$$M_D = \frac{M_Z - y_Z M_T}{x_Z - y_Z} \qquad (5)$$

Thus, the true bridging liquid to solid ratio is given:

$$TBSR = \frac{V_D}{V_S} = \frac{\frac{M_D}{\rho_D}}{\frac{M_S}{\rho_S}} \qquad (6)$$

If the phase is considered to be an ideal solution, ρ_D can be estimated as:

$$\frac{1}{\rho_D} = \sum \left(\frac{x_i}{\rho_i}\right) \qquad (7)$$

3. Materials and methods

3.1. Materials

A summary of literature values for the interfacial tension of different bridging liquids in water is displayed in Table 2. These values provided an insight for which bridging liquids have the highest miscibility in spherical agglomeration systems. Solvents were selected based upon those which have general agreement across a variety of publications.

3.2. Experimental determination of ternary phase diagrams

Experiments were conducted at room temperature, 19.5 °C (± 0.5 °C). Solutions of acetone and one of the bridging liquids were prepared and thoroughly mixed, with varying compositions between 5% w/w and 95% w/w acetone, in conical flasks to a total mass of 20 g. Distilled water was added dropwise from a burette whilst the flask was agitated vigorously by hand. At the onset of a cloudy solution, two immiscible phases were present. Solutions were allowed to separate without agitation for ten seconds. If both immiscible phases were observed visually through a separation layer, the titration was considered complete. The mass of water added to the solution was recorded. A further two repeats following the same methodology were performed. Nineteen conditions of triplicates produced fifty-seven data points. This produced the first half of the binodal curve, i.e. the curve which separates miscible and immiscible regions.

To obtain the second half of the binodal curve, solutions of water and acetone were prepared in varying compositions between 40 and 90% w/w water and titrated dropwise with the required bridging liquid. The first solution contained 8 g (40% w/w) of water and 12 g (60% w/w) of acetone. This yielded a further eighteen data points of immiscible systems for each bridging liquid. As the mass of all components was known at each stage, the final composition at the titration end point was calculated in terms of mass fractions. The data was then plotted on ternary phase diagrams (one for each bridging liquid).

Experimental results for determination of ternary phase diagrams

Table 3
Chemical and physical properties of chemicals used at 1 atm and 25 °C [43].

Chemical Species	Molecular Formula	Molecular Weight	Density
(−)	(−)	(g mol^{-1})	(g cm^{-3})
Acetone	C_3H_6O	58.079	0.7845
Chloroform	$CHCl_3$	119.378	1.4788
Heptane	C_7H_{16}	100.202	0.6795
MIBK	$C_6H_{12}O$	100.158	0.7965
Butyl acetate	$C_6H_{12}O_2$	116.158	0.8825[a]
Salicylic acid	$C_7H_6O_3$	138.121	1.4430[a]
Toluene	C_7H_8	92.139	0.8668[a]
Water	H_2O	18.015	0.9970

[a] Values at 20 °C.

Table 2
Experimental interfacial tension data of bridging liquids in water at 1 atm and 25 °C.

	Chloroform	Heptane	MIBK	Butyl acetate	Toluene	Reference
	30.8	50.1	10.4	–	35.4	[37]
	31.6	50.2	–	14.5	36.1	[38]
Interfacial Tension in Water at 25 °C	32.8[a]	50.2	10.1	14.5	36.1	[39]
(dyne cm^{-1})	31.6	50.2	10.1	14.5	36.1	[40]
	31.1	50.1	–	–	35.8	[41]
	–	–	–	15.0[b]	35.8[b]	[42]

[a] Values at 20 °C.

[b] Values at 17 °C. Acetone (≥ 99.8%) was purchased from Sigma-Aldrich (UK) for use as the solvent. Bridging liquids of chloroform (99+ %), heptane (99%) and toluene (99.8%) were also purchased from Sigma-Aldrich. 4-Methyl-2-pentanone (MIBK, 99.5%) and butyl acetate (99+ %) were purchased from Acros Organics (UK) and were also used as bridging liquids. Salicylic acid was purchased from Sigma Aldrich and was used as received. Distilled water prepared locally was used as an anti-solvent. Important chemical and physical properties for these components are listed in Table 3.

showed a high level of reproducibility. A summary of the results for all five bridging liquid solvents is presented in Fig. 4. It is critical to identify the boundary between miscible and immiscible regions, as spherical agglomeration is optimal within the immiscible region where two distinct phases are present. Generally, the data follows a smooth curve for the mass fraction data, which defines the aforementioned boundary.

3.3. Computational determination of ternary phase diagram

Aspen Plus (v8.4, Aspen Technology, USA) was used to simulate the ternary phase diagram for all the bridging liquids investigated. This allowed the tie-lines of each ternary phase diagram to be found. Tie-lines define an equilibrium of the two immiscible phases and allow the composition of each phase to be identified. The location of an agglomerating system on a tie-line also provides the relative mass fractions of each immiscible phase.

Simulations were conducted using UNIFAC, UNIF-LL, UNIQ-RK and UNIQUAC models for each solvent. The former three of these models are variations on the UNIQUAC model, which itself is built upon the activity coefficients of chemical species [44]. This, in turn, is directly related to the functional groups of each solvent species molecule. The activity coefficient also accounts for the non-ideal behaviour upon mixing of the three solvent components. The simulations used liquid-liquid phases only at 19.5 °C and 1.01325 bar (1 atm). Twenty-five tie-lines were obtained for each bridging liquid system. The maximum number of iterations was set to five thousand, with an error tolerance of 1×10^{-5}. Additional ties were then created by interpolation. Full details of the method are given in [45].

3.4. Agglomeration experiments

For the agglomeration experiments, salicylic acid saturated mother solutions were prepared in the following compositions: 95% *w/w* water, 5% w/w acetone; 90% w/w water, 10% w/w acetone; 85% w/w water, 15% w/w acetone.

To ensure the immersion mechanism occurred, primary particles were required to be as small as possible. For preparation of the primary crystals, salicylic acid was sieved using a 45 μm sieve and pan on a Retsch Sieve-shaker (AS200, Retsch, Germany). An amplitude of 2.25 mm was used for five minutes to ensure breakage of primary crystals and recovery of crystals <45 μm. These samples were recovered and set aside.

12 g of prepared salicylic acid was suspended in the saturated mother solution (388 g) in a sealed reactor of 1 L. This corresponds to a 3% w/w loading. The system was agitated for one minute at 750 rpm, using a Rushton turbine, to disperse the solid within the saturated solution. After this point, infusion of the required amount of bridging liquid occurred. The bridging liquid solvent was poured through a funnel into the top of the reactor. This represents an infusion time of sub-one second. Post-infusion, agitation of the system continued until a total time of 45 min was reached. Each experiment was performed in triplicate.

To analyse the percentage of crystals agglomerated upon experimental completion, the agglomeration suspensions were filtered after 45 min, using glass microfibre filter papers with a pore size of 1.2 μm. The retentate was allowed to dry overnight at room temperature. The sample was then sieved using a variety of different sieve meshes on the sieve shaker, at an amplitude of 0.40 mm for 30 s. This time is used to avoid the breakage and/or attrition of agglomerates. The smallest mesh used was 300 μm and the largest mesh used was 8 mm. The agglomerate mass retained in each sieve was recorded and a particle size distribution determined for each experiment. Particles which passed through all sieve meshes were recovered from the pan (< 300 μm) and are subsequently considered un-agglomerated fines.

4. Results and discussion

4.1. Ternary phase diagrams

The experimental titration results are shown in Fig. 4 for water-acetone-bridging liquid systems. The onset of turbidity during each titration was easily observed, and this is reflected in the high level of reproducibility across all the bridging liquids. The general shape of all systems, regardless of the bridging liquid used, follows a smooth, bell-shaped curve with shallow sides. The height of the curve represents the degree of the miscibility of the three solvents. Less miscible bridging liquids can be identified by a higher peak in the curve, or a greater area in the immiscible region. Broadly speaking, bridging liquids with higher surface tension have a larger immiscible region (see Table 2). Heptane displays the highest peak, followed by toluene, chloroform, butyl-acetate, and MIBK.

Five thermodynamic models were compared to experimental results; UNIQUAC, and its variations UNIFAC, UNIF-LL, UNIQ-RK. Each model was simulated against all five bridging liquids, and the results compared. The models with the closest alignment to the experimental results are displayed in Fig. 4.

UNIF-LL was shown to best predict water-acetone-chloroform systems, whilst UNIFAC best predicted water-acetone-heptane systems. UNIQUAC was found to best predict the behaviour of the remaining systems: butyl acetate; MIBK; toluene. For butyl acetate and MIBK, the interfacial tension in water is relatively low. Subsequently, there is a much higher degree of miscibility, and the system behaviour is more difficult to predict with a poorer match between experimental data and the model for peak height.

4.2. Comparison of TBSR with BSR for all systems

Fig. 5 shows calculated TBSR values as a function of BSR for all systems studied at 3% w/w solids loading. The TSBR values are calculated from eqns.4–7 and the ternary phase diagrams. To reach the formation of two immiscible phases, the solubility of the bridging liquid in the bulk solution must be exceeded. At low BSR, the system is completely miscible and TBSR = 0. When the immiscible phases do form, some soluble volume is lost to the bulk solution. As result of this behaviour, TBSR is always less than the BSR for low BSR values. Bulk solutions with a higher initial mass fraction of water have least deviation from the BSR = TBSR relationship, as all the bridging liquids are much less miscible in water, compared to acetone. As the initial mass fraction of acetone is increased, significant deviation of TBSR from the BSR occurs, regardless of the bridging liquid used. In the ternary phase diagram, this is reflected by theoretical systems requiring more bridging liquid to cross the binodal curve into the immiscible region of the diagram.

The relationship between TBSR and BSR varies widely depending on the system used and the position on the phase diagram. Consider the systems shown in Fig. 5. To achieve a TBSR of 0.5, the required BSR varies from 0.5 (heptane; 95 %W/5%A) to 2 (MIBK; 95%A/5 %W). This is consistent with the wide range of reported optimum BSR values in the literature (Fig. 2). It is interesting to note in Fig. 2 that the completely immiscible and insoluble model system (kerosene/water/CaCO₃) gives agglomeration at the lowest BSR values (0.05–0.35). For this system, by definition TSBR = BSR. Other partially miscible systems reported show larger BSR values.

Interestingly, the chloroform system shows a slightly different trend as the proportion of acetone is increased. This was the only system studied where the tie-lines within the ternary phase diagram have a negative gradient, (Fig. 4c). This negative gradient means that a much larger transfer of acetone from the initial bulk solution to the binder rich phase can occur, even at very low bridging liquid addition levels.

Fig. 6 and Fig. 7 shows the impact TBSR-BSR relationship of solids loading in the range 1–5% w/w for two of the systems studied. There is a
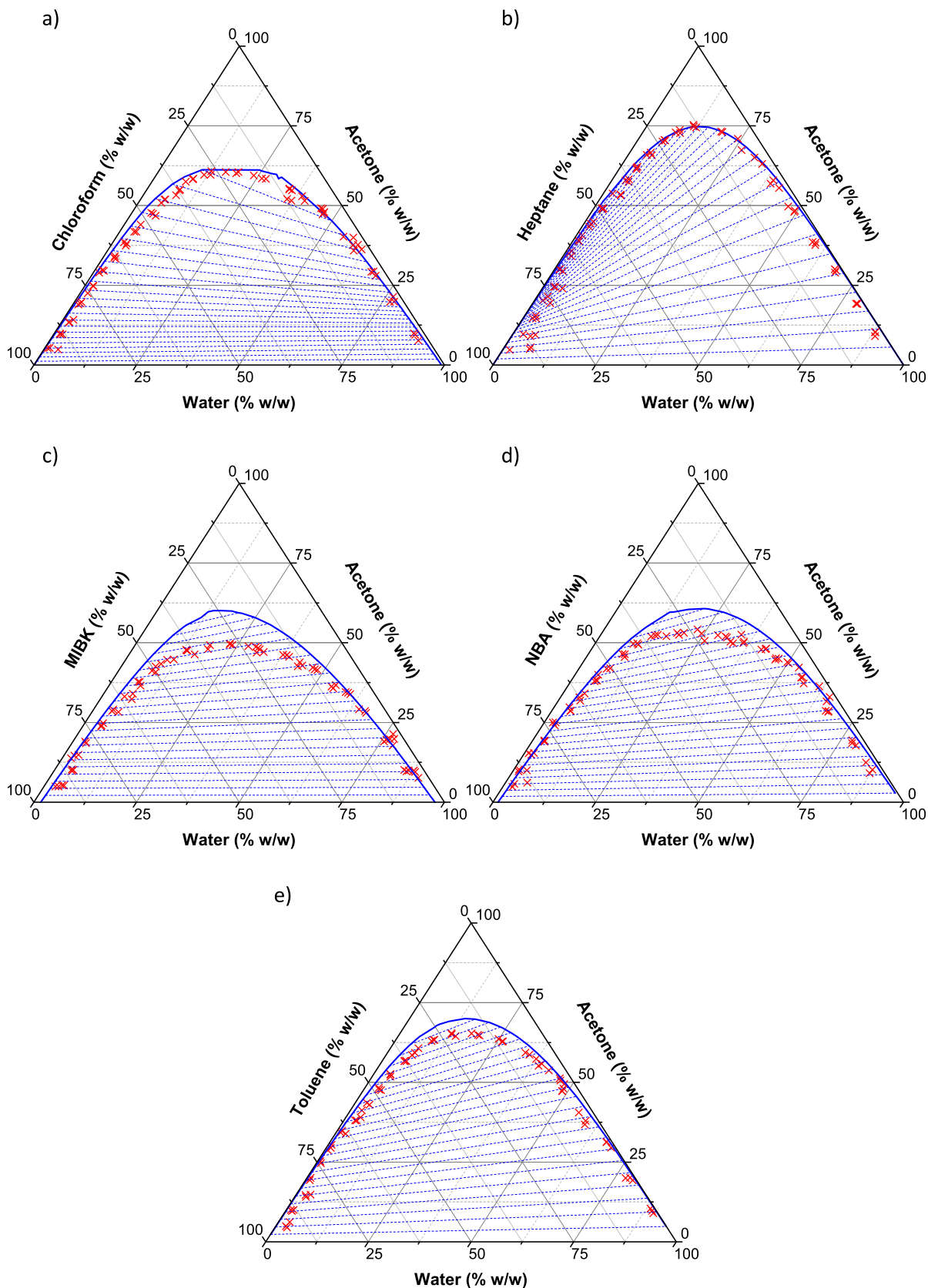
Fig. 4. Ternary phase diagrams (% *w*/w) of water-acetone-bridging liquid systems with experimental data and Aspen prediction overlay: **a)** chloroform UNIF-LL prediction; **b)** heptane UNIFAC prediction; **c)** MIBK UNIQUAC prediction; **d)** butyl acetate UNIQUAC prediction; **e)** toluene UNIQUAC prediction.
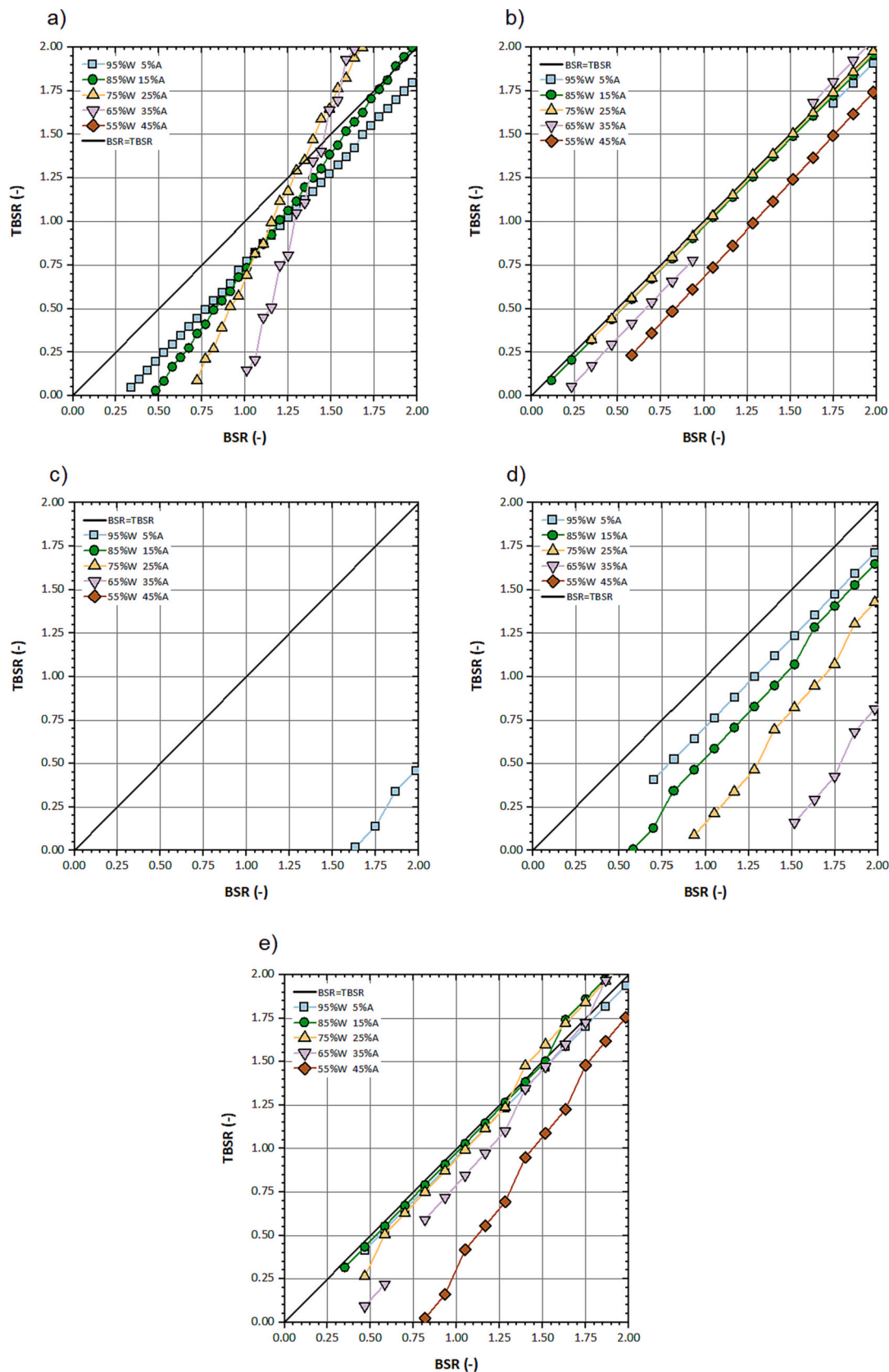
Fig. 5. BSR vs TBSR of water-acetone-bridging liquid systems **a)** heptane; **b)** toluene; **c)** chloroform; **d)** *n*-butyl acetate; **e)** MIBK.
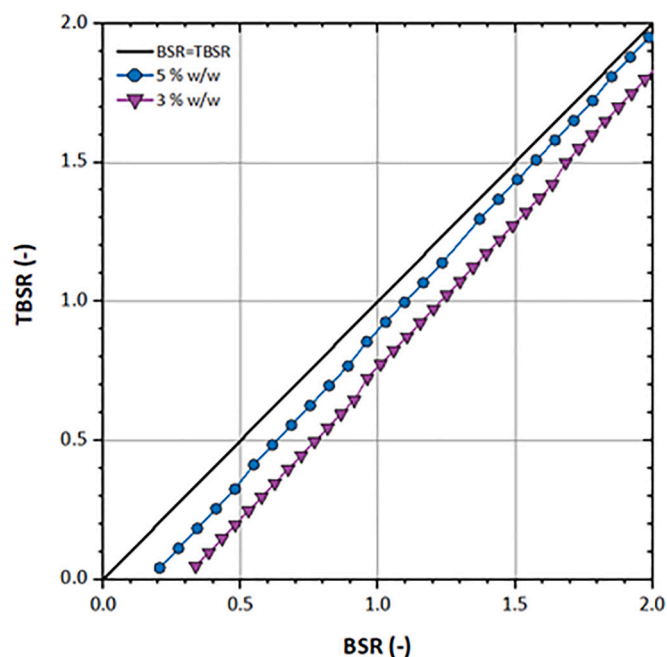
Fig. 6. Comparison between a solid loading of 3% *w/w* and 5% w/w for 95% w/w, 5% w/w acetone systems, with chloroform as the bridging liquid.

Fig. 8. Increasing the bridging liquid volume addition as solids loading increases causes the system to move further into the immiscible region, shown here for four example bulk solution conditions.

operating point is very close to the boundary envelope, then a small drop in solids content could cause a dramatic change in performance.

An important observation from this analysis is that for a given ternary solvent system, there is no single value of BSR that is optimum. Changes to the amount of antisolvent added or different solids loading will move the operating point on the ternary phase diagram, changing the proportion of added binder liquid that is actually available for agglomeration. This is shown in Fig. 8. Small changes in operating conditions that can occur during scale up or manufacturing operation could lead to significant changes in performance. The potential impact can be minimised by using a binder/solvent antisolvent system with high immiscibility, and high solids loading. However, choice of the system and operating point may be constrained by upstream and downstream requirements. The optimum TSBR will be much less dependent on operating system and is therefore a better parameter to target during design and scale up.

4.3. Preliminary Experimental Validation of TBSR as a unifying parameter

Simple salicylic acid agglomeration experiments were conducted for three of the systems studied (chloroform, MIBK and n-butyl acetate) at two different compositions of water/acetone for MIBK and n-butyl acetate (95%/5% and 90%/10%) and three for chloroform (95%/5%; 90%/10%; 85%/15%). Both the amount of un-agglomerated fines, and the agglomerate size distribution results were measured.

Fig. 9 shows the amount of un-agglomerated fines as a function of BSR (filled data points) and TSBR (unfilled data points). In these experiments, the amount of un-agglomerated fines are low and generally decrease with increasing BSR/TSBR as expected. However, the value of BSR to achieve a given extent of agglomeration vary widely depending on the chosen bridging liquid and solvent composition in the range of 0.3–2.0. There is no unifying relationship between agglomeration extent and BSR. In contrast, all data lies in a narrow range of TBSR from 0.05 to 0.15.

Fig. 10 shows agglomerate mean size as a function of BSR/TBSR. The agglomerate size distributions, for all bridging liquids and mother solution compositions, show an increase in agglomerate size with an
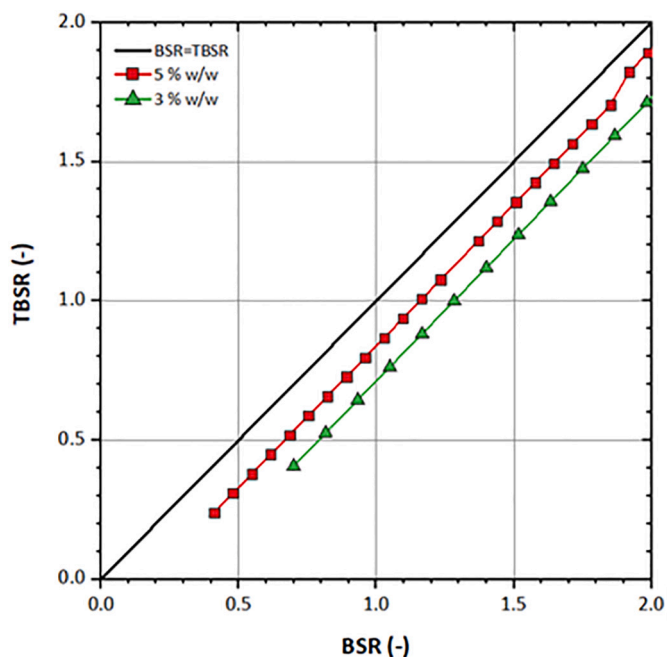

Fig. 7. Comparison between a solid loading of 3% w/w and 5% w/w for 95% w/w, 5% w/w acetone systems, with n-butyl acetate as the bridging liquid.

dramatic effect of solids loading. For example, in the chloroform system, to achieve a TBSR of 0.5 requires a BSR of 1.3 at 1% solids loading but only 0.6 at 5% solids loading. Keeping BSR constant when changing solids loading can lead to a considerable difference in the true amount of binding phase available for agglomeration, especially at low solids loading. At 1% w/w, for the *n*-butyl acetate system, the operating point is very close to the fully miscible region, so that very little of the added binder is actually available for agglomeration. Increasing the solids content increases the amount of bridging liquid added and pushes the operating point further into the immiscible region (see Fig. 8). If the
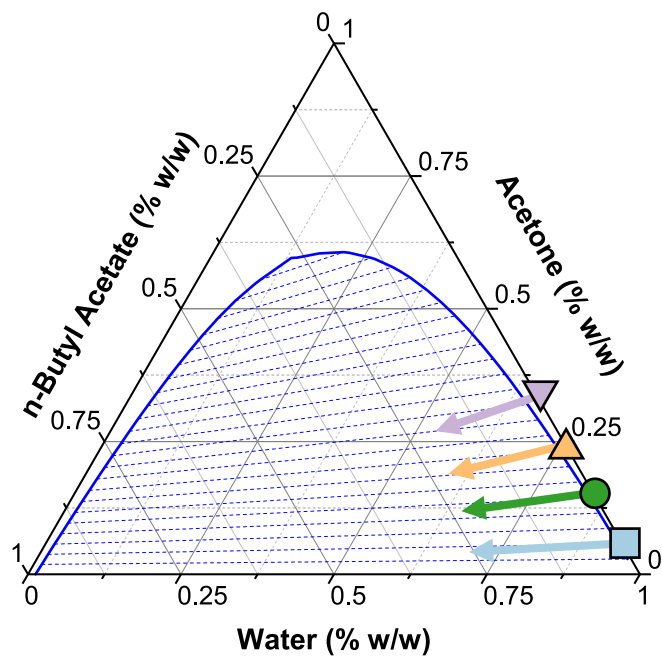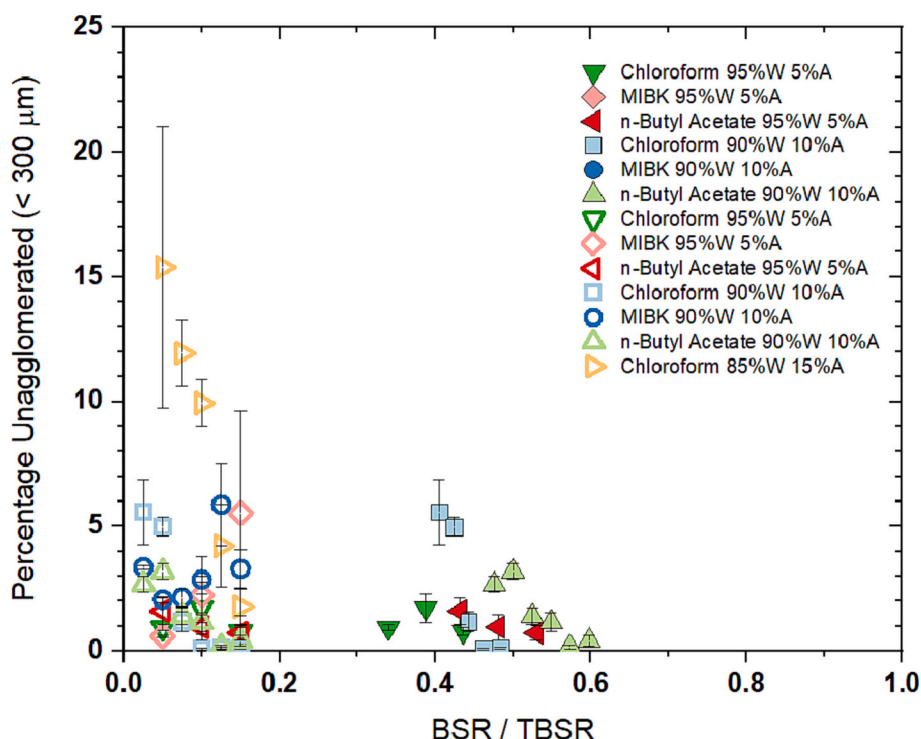
Fig. 9. The relationship between the BSR/TBSR with the percentage of fines observed for the systems investigated. BSR showed as filled data points. TBSR shown as unfilled data points.
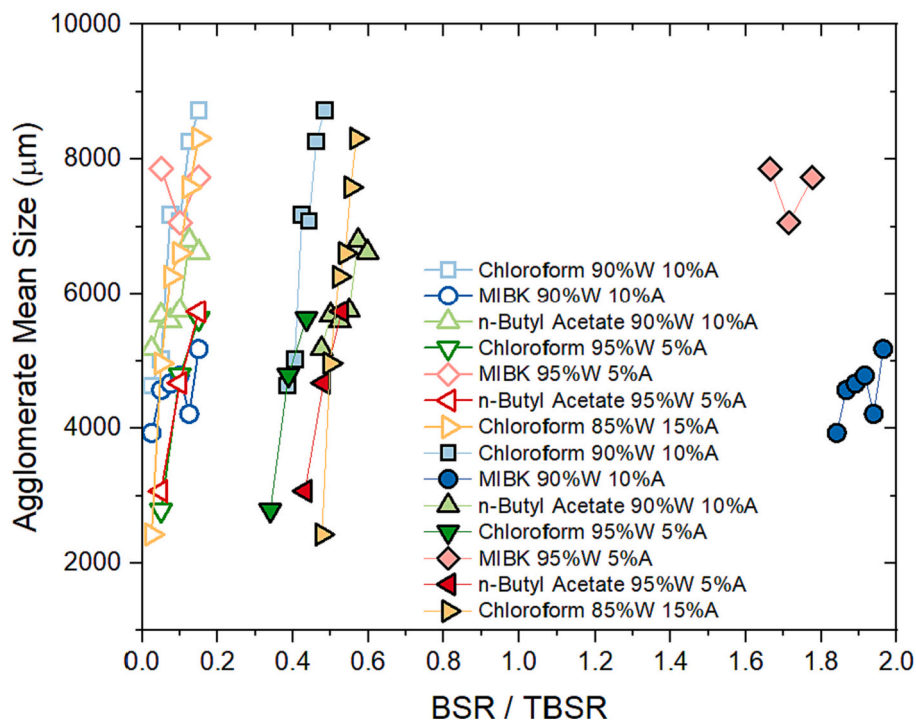

Fig. 10. The relationship between the BSR/TBSR and the agglomerate mean size for different bridging liquids and bulk solutions. BSR showed as filled data points. TBSR shown as unfilled data points.

increasing BSR/TBSR value. For each system, the agglomerate size is very sensitive to BSR, but the optimum value of BSR is different for each system studied over a wide range. In contrast, for all systems, the relationship between agglomerate size and TSBR is much less sensitive to the system studied.

The TBSR values calculated here are lower than would be expected based on the analogy to wet granulation but consistent with those reported for the model kerosene-water-CaCO₃ and shown in Fig. 2. Other system properties such as the contact angle between the binder liquid and the crystals and the binder liquid viscosity, will also impact the

system thermodynamics and kinetics. Further data for more systems and over a wider range of TBSR and agglomeration process conditions is needed for full validation. Nevertheless, these data strongly indicate that TBSR is a useful design and scale up parameter for spherical agglomeration.

5. Conclusions

The bridging liquid-solid ratio (BSR) is a very important parameter in spherical agglomeration There is a narrow critical range for BSR, within which agglomerates with the desired mechanical properties are formed. The literature shows that the optimum BSR is highly system dependent for pharmaceutical systems. Our analysis shows this effect can be explained by the partial miscibility of binder liquids with the solvent/antisolvent bulk solution which reduces the actual volume of dispersed binder rich phase available for agglomeration. Furthermore, no system has a single optimum value of BSR. Rather, it depends on the position on the ternary phase diagram set by the solvent/antisolvent ratio and the solids loading in the system. These factors are typically set by the upstream crystallisation step and can vary during scale up and transfer to manufacturing.

The true bridging liquid-solid ratio (TBSR) defined in this paper is based on the actual amount of dispersed bridging liquid rich phase available for agglomeration. It is therefore much more robust to use as a design parameter. Preliminary experimental validation shows agglomeration success tracks reasonably well with TSBR, independent of the system chosen. TSBR is clearly defined and easily calculated provided the solvent-antisolvent-binder liquid ternary phase diagram is available. The definition allows a simple comparison between different spherical agglomeration systems with different bridging liquids. Thus, TBSR is recommended as a dimensionless design and scaling parameter for spherical agglomeration behaviour in the way liquid saturation is used in wet granulation systems. Caution should be taken, as whilst evaluation of solvent miscibility allows greater process performance prediction in spherical agglomeration, other factors such solvent wettability with the crystal phase should also be considered. Experimental validation over a wider range of operating conditions and crystal systems is still required. However, the new definition shows promise as the basis for the development of a dimensionless regime map in which spherical agglomeration process performance can be accurately predicted. Ultimately, such a regime map is imperative for engineers to develop robust processes and may improve the industrial adoption of the technique as a whole.

CRediT authorship contribution statement

Jonathan D. Tew: Conceptualization, Methodology, Validation, Formal analysis, Investigation, Writing – original draft, Visualization. **Kate Pitt:** Conceptualization, Writing – review & editing, Visualization, Supervision. **Rachel Smith:** Conceptualization, Writing – review & editing, Visualization, Supervision, Funding acquisition. **James D. Litster:** Conceptualization, Writing – review & editing, Visualization, Supervision, Funding acquisition.

Declaration of Competing Interest

The authors declare that they have no known competing financial interests or personal relationships that could have appeared to influence the work reported in this paper.

Data availability

Data will be made available on request.

References

[1] Y. Kawashima, M. Okumura, H. Takenaka, Spherical crystallization: direct spherical agglomeration of salicylic acid crystals during crystallization, Science. 216 (4550) (1982) 1127–1128.

[2] B. Shekunov, P. York, Crystallisation processes in pharmaceutical technology and drug delivery, J. Cryst. Growth 211 (14) (2000) 122–136.

[3] Y. Kawashima, M. Imai, H. Takeuchi, H. Yamamoto, K. Kamiya, T. Hino, Improved flowability and compactibility of spherically agglomerated crystals of ascorbic acid for direct tableting designed by spherical crystallization process, Powder Technol. 130 (1–3) (2003) 283–289.

[4] M. Maghsoodi, A.S. Tajalli Bakhsh, Evaluation of physico-mechanical properties of drug-excipients agglomerates obtained by crystallization, Pharm. Dev. Technol. 16 (3) (2011) 243–249.

[5] S.M. Iveson, J.D. Litster, K. Hapgood, B.J. Ennis, Nucleation, growth and breakage phenomena in agitated wet granulation processes: a review, Powder Technol. 117 (1–2) (2001) 3–39.

[6] R. Peña, Z.K. Nagy, Process intensification through continuous spherical crystallization using a two-stage mixed suspension mixed product removal (MSMPR) system, Crystal. Growth Design. 15 (9) (2015) 4225–4236.

[7] C. Subero-Couroyer, D. Mangin, A. Rivoire, A.F. Blandin, J.P. Klein, Agglomeration in suspension of salicylic acid fine particles: analysis of the wetting period and effect of the binder injection mode on the final agglomerate size, Powder Technol. 161 (2) (2006) 98–109.

[8] Y. Kawashima, K. Furukawa, H. Takenaka, The physicochemical parameters determining the size of agglomerate prepared by the wet spherical agglomeration technique, Powder Technol. 30 (2) (1981) 211–216.

[9] K. Pitt, R. Peña, J.D. Tew, K. Pal, R. Smith, Z.K. Nagy, et al., Particle design via spherical agglomeration: a critical review of controlling parameters, rate processes and modelling, Powder Technol. 326 (2018).

[10] Y. Kawashima, Y. Kurachi, H. Takenaka, Preparation of spherical wax matrices of sulfamethoxazole by wet spherical agglomeration technique using a CMSMPR agglomerator, Powder Technol. 32 (2) (1982) 155–161.

[11] Y. Kawashima, M. Okumura, H. Takenaka, The effects of temperature on the spherical crystallization of salicylic acid, Powder Technol. 39 (1) (1984) 41–47.

[12] S.K. Pagire, S.A. Korde, B.R. Whiteside, J. Kendrick, A. Paradkar, Spherical crystallization of carbamazepine/saccharin co-crystals: selective agglomeration and purification through surface interactions, Crystal. Growth Design. 13 (10) (2013) 4162–4167.

[13] H. Zhang, Y. Chen, J. Wang, J. Gong, Investigation on the spherical crystallization process of cefotaxime sodium, Ind. Eng. Chem. Res. 49 (3) (2010) 1402–1411.

[14] K. Morishima, Y. Kawashima, Y. Kawashima, H. Takeuchi, T. Niwa, T. Hino, Micromeritic characteristics and agglomeration mechanisms in the spherical crystallization of bucillamine by the spherical agglomeration and the emulsion solvent diffusion methods, Powder Technol. 76 (1) (1993) 57–64.

[15] J. Thati, C. Rasmuson, Particle engineering of benzoic acid by spherical agglomeration, Eur. J. Pharm. Sci. 45 (5) (2012) 657–667.

[16] A.F. Blandin, D. Mangin, A. Rivoire, J.P. Klein, J.M. Bossoutrot, Agglomeration in suspension of salicylic acid fine particle: influence of some process parameters on kinetics and agglomerate final size, Powder Technol. 130 (1) (2003) 316–323.

[17] D. Amaro-González, B. Biscans, Spherical agglomeration during crystallization of an active pharmaceutical ingredient, Powder Technol. 128 (2–3) (2002) 188–194.

[18] J. Thati, C. Rasmuson, On the mechanisms of formation of spherical agglomerates, Eur. J. Pharm. Sci. 42 (4) (2011) 365–379.

[19] Y. Kawashima, M. Okumura, H. Takenaka, A. Kojima, Direct preparation of spherically agglomerated salicylic acid crystals during crystallization, J. Pharm. Sci. 73 (11) (1984) 1535–1538.

[20] A.R. Paradkar, A.P. Pawar, J.K. Chordiya, V.B. Patil, A.R. Ketkar, Spherical crystallization of celecoxib, Drug Dev. Ind. Pharm. 28 (10) (2002) 1213–1220.

[21] A.N. Usha, S. Mutalik, M.S. Reddy, A.K. Ranjith, P. Kushtagi, N. Udupa, Preparation and, in vitro, preclinical and clinical studies of aceclofenac spherical agglomerates, Eur. J. Pharm. Biopharm. 70 (2) (2008) 674–683.

[22] Y. Kawashima, S. Aoki, H. Takenaka, Spherical agglomeration of aminophylline crystals during reaction in liquid by the spherical crystallization technique, Chem. Pharm. Bull. 30 (5) (1982) 1900–1902.

[23] S. Wu, K. Li, T. Zhang, J. Gong, Size control of atorvastatin calcium particles based on spherical agglomeration, Chem. Eng. Technol. 38 (6) (2015) 1081–1087.

[24] J. Katta, Å.C. Rasmuson, Spherical crystallization of benzoic acid, Int. J. Pharm. Vol. 348 (2008) 61–69.

[25] M. Leane, K. Pitt, G. Reynolds, J. Anwar, S. Charlton, A. Crean, et al., A proposal for a drug product manufacturing classification system (MCS) for oral solid dosage forms, Pharm. Dev. Technol. 20 (1) (2015) 12–21.

[26] L.X. Liu, I. Marziano, A.C. Bentham, J.D. Litster, E.T. White, T. Howes, Influence of particle size on the direct compression of ibuprofen and its binary mixtures, Powder Technol. 240 (2013) 66–73.

[27] R. Petela, Prediction of the product size in the agglomeration of coal particles in a water-oil emulsion, Fuel. 70 (4) (1991) 509–517.

[28] A.F. Blandin, D. Mangin, C. Subero-Couroyer, A. Rivoire, J.P. Klein, J. M. Bossoutrot, Modelling of agglomeration in suspension: application to salicylic acid microparticles, Powder Technol. 156 (1) (2005) 19–33.

[29] M. Ritala, P. Holm, T. Schaefer, H.G. Kristensen, Influence of liquid bonding strength on power consumption during granulation in a high shear mixer, Drug Dev. Ind. Pharm. 14 (8) (1988) 1041–1060.

[30] J. Litster, Design and Processing of Particulate Products [Internet], Cambridge University Press, 2016 [cited 2023 Apr 24]. Available from: https://www.cambridge.org/core/product/identifier/9781139017558/type/book.

[31] A.S. Bos, F.J. Zuiderweg, Kinetics of continuous agglomeration in suspension, Powder Technol. 44 (1) (1985) 43–51.

[32] P. Di Martino, C. Barthélémy, F. Piva, E. Joiris, G.F. Palmieri, S. Martelli, Improved dissolution behavior of fenbufen by spherical crystallization, Drug Dev. Ind. Pharm. 25 (10) (1999) 1073–1081.

[33] A. Sano, T. Kuriki, T. Handa, H. Takeuchi, Y. Kawashima, Particle design of tolbutamide in the presence of soluble polymer or surfactant by the spherical crystallization technique: improvement of dissolution rate, J. Pharm. Sci. 76 (6) (1987) 471–474.

[34] J. Varshosaz, N. Tavakoli, F.A. Salamat, Enhanced dissolution rate of simvastatin using spherical crystallization technique, Pharm. Dev. Technol. 16 (5) (2011) 529–535.

[35] S. Jitkar, R. Thipparaboina, R.B. Chavan, N.R. Shastri, Spherical agglomeration of platy crystals: curious case of etodolac, Crystal. Growth Design. 16 (7) (2016) 4034–4042.

[36] K. Ikegami, Y. Kawashima, H. Takeuchi, H. Yamamoto, N. Isshiki, D.I. Momose, et al., Simultaneous particulate design of primary and agglomerated crystals of steroid by spherical agglomeration in liquid for dry powder inhalation, Powder Technol. 130 (1–3) (2003) 290–297.

[37] H.M. Backes, M. Jing Jun, E. B, G. M. Interfacial tensions in binary and ternary liquid-liquid systems, Chem. Eng. Sci. 45 (1) (1990) 275–286.

[38] D.J. Donahue, F.E. Bartell, The boundary tension at water-organic liquid interfaces, J. Phys. Chem. 56 (4) (1952) 480–484.

[39] A.A. Freitas, F.H. Quina, F.A. Carroll, Estimation of water−organic interfacial tensions. A linear free energy relationship analysis of interfacial adhesion, J. Phys. Chem. B 101 (38) (1997) 7488–7493.

[40] F.U. Jufu, L.I. Buqiang, W. Zihao, Estimation of fluid-fluid interfacial tensions of multicomponent mixtures, Chem. Eng. Sci. 41 (10) (1986) 2673–2679.

[41] B. Li, J. Fu, Interfacial tensions of two-liquid-phase ternary systems, J. Chem. Eng. Data 37 (2) (1992) 172–174.

[42] M.Z. Shahid, M.R. Usman, M.S. Akram, S.Y. Khawaja, W. Afzal, Initial interfacial tension for various organic-water systems and study of the effect of solute concentration and temperature, J. Chem. Eng. Data 62 (4) (2017) 1198–1203.

[43] D.R. Lide, CRC Handbook of Chemistry and Physics 86th Edition 2005-2006, CRC Press, 2005.

[44] A. Fredenslund, R.L. Jones, J.M. Prausnitz, Group-contribution estimation of activity coefficients in nonideal liquid mixtures, AICHE J. 21 (6) (1975) 1086.

[45] J.D. Tew, Spherical Agglomeration for Intensified Pharmaceutical Manufacturing: Evaluating the Influence of Bridging Liquid Miscibility, 2021.